T4:

Stellar Masers *Chair: Elizabeth Humphreys*

https://doi.org/10.1017/S1743921312006977 Published online by Cambridge University Press

Cosmic Masers - from OH to H_0
Proceedings IAU Symposium No. 287, 2012
R.S. Booth, E.M.L. Humphreys & W.H.T. Vlemmings, eds.

doi:10.1017/S1743921312006977

Masers in evolved star winds

Anita M. S. Richards

UK ARC Node, JBCA, School of Physics and Astronomy, University of Manchester, UK
email: amsr@jb.man.ac.uk

Abstract. This review summarises current observations of masers around evolved stars and models for their location and behaviour, followed by some of the many highlights from the past 5 years. Some of these have been the fruition of long-term monitoring, a vital aspect of study of stars which are both periodically variable and prone to rapid outbursts or transition to a new evolutionary stage. Interferometric imaging of masers provide the highest-resolution probes of the stellar wind, but their exponential amplification and variability means that multiple observations are needed to investigate questions such as what drives the wind from the stellar surface; why does it accelerate slowly over many tens of stellar radii; what causes maser variability. VLBI parallaxes have improved our understanding of individual objects and of Galactic populations. Masers from wide range of binary and post-AGB objects are accessible to sensitive modern instruments, including energetic symbiotic systems. Masers have been detected up to THz frequencies with *Herschel* and ALMA's ability to resolve a wide range of maser and thermal lines will provide accurate constraints on physical conditions including during dust formation.

Keywords. masers, surveys, stars: distances, late-type, evolution, AGB and post-AGB, supergiants, binaries: symbiotic, Galaxy: kinematics and dynamics

1. Introduction

Circumstellar masers are most abundant around solitary Asymptotic Giant Branch (AGB) and Red Supergiant (RSG) stars. The former had main sequence precursors < 8 $M_\odot$, the latter are more massive. Both have depleted hydrogen in their outer layers, swollen to between $\sim 1 - 10$ AU or more in diameter, RSG being roughly ten times larger than AGB stars. Their surface temperatures are $\sim 2000 - 3500$ K, RSG being at the hotter end of the range. They exhibit deep pulsations with periods P ranging from $\leqslant 0.5$ yr for low-mass semi-regular (SR) and Mira variables, to several years for the thickest-shelled OH/IR stars and supergiants. Molecules form in the stellar atmosphere and mass loss is copious, from $\sim 10^{-7}$ to $> 10^{-5}$ $M_\odot$ yr^{-1} depending on mass, age and metallicity. In this context 'solitary' means the absence of any companion detectable directly or by a kinematic signature; the distended stellar surfaces do not show any rotation and the gently expanding winds allow masers to propagate very efficiently in all directions. It has been traditional to present a cartoon of stellar mass loss traced by masers, but it is now possible to illustrate the process directly from observations, Fig. 1.

There are many open questions even in solitary star evolution, discussed in Section 2. Some of the advances in precise distance measurements are summarised in Section 3. Masers have also been detected from binary or possibly binary objects and I will describe some dramatic recent discoveries in Section 4. The masers accessible to cm-wave radio telescopes are those found in O-rich circumstellar envelopes (CSEs), i.e. SiO, H_2O and OH. (Sub-)mm wave masers include higher transitions of SiO and H_2O and also species found in C-rich CSEs, summarised in Section 5.

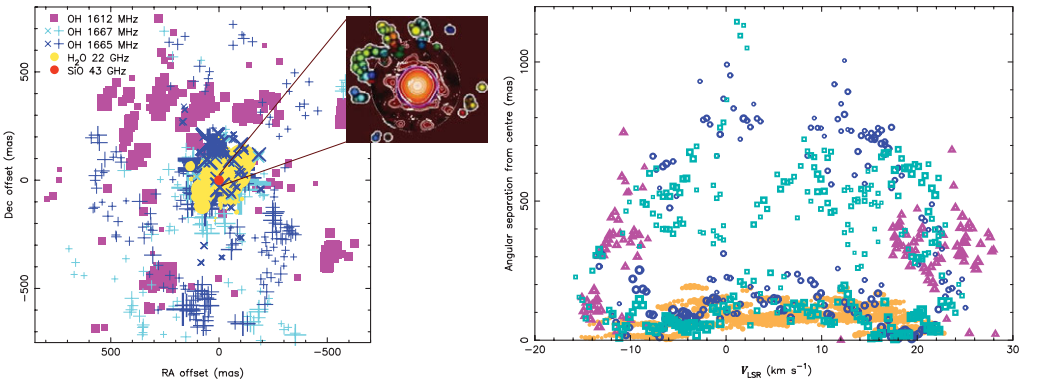

Figure 1. The inset shows the stellar disc of VX Sgr, resolved at 2μm by Chiavassa *et al.* (2010) overlaid with SiO masers mapped by Chen *et al.* (2006). The larger-scale structure traced by H_2O (Murakawa *et al.* 2003) and OH masers is shown on the left. The angular separation of the H_2O and OH masers from the assumed stellar position, as a function of $V_{\rm LSR}$, is shown on the right.

2. The origin and acceleration of stellar winds

2.1. *Acceleration*

Bowen (1988) modelled the AGB mass loss process initiated by the levitation of material by stellar pulsations, to the point where dust forms and radiation pressure on grains accelerates the wind away from the star, imparting momentum to the gas by collisions. However, Woitke (2006) cast doubt on whether silicate-based grains could form close enough to the star for this process to be effective in O-rich stars. IR interferometry (e.g. Danchi *et al.* 1994) showed the inner rim of the silicate dust shell is typically at $\geqslant 5$ stellar radii ($R_\star$). The dust must form promptly, since the collision rate is too slow for grains to grow outside this radius, but Chapman & Cohen (1986) found that the wind traced by all maser species accelerates gradually out to $\sim 100R_\star$ in VX Sgr (Fig. 1). This was also seen for e.g. S Per (Richards *et al.* 1999a), IK Tau, RT Vir, U Her and U Ori (Bains *et al.* 2003). The wind is accelerated through escape velocity as it traverses the H_2O maser shell (Yates & Cohen 1994) and larger shells have higher velocities but follow a similar gradient, Fig. 2. *Herschel* results also provide evidence for gradual acceleration. Lines from higher excitational states, emanating from closer to the star, have narrower velocity widths than those produced under cooler conditions (Decin *et al.* 2010).

2.2. *Maser beaming*

The position and size of individual maser spots is measured by fitting 2-D Gaussian components, uncertainty proportional to (beamsize)/(signal-to-noise ratio), and hence can achieve sub-mas (often sub-AU) accuracy for bright masers. The measured size is often much smaller than the true size of the emitting region. The spots often form series, with a Gaussian spectral profile and systematic position increments. If the spot positions are spatially resolved (as is the case for MERLIN observations of 22-GHz H_2O masers) the total extent of such features represent the physical size of maser clumps. In such cases, (component size)/(feature size) gives a direct estimate of the maser beaming angle (Strelniskii these proceedings; (Richards *et al.* 2011)). The arrangements of components within clouds can sometimes be traced from epoch to epoch in proper motion studies (Richards *et al.* 1999b; 2012), twisting and distorting at approximately the local sound speed.

https://doi.org/10.1017/S1743921312006977 Published online by Cambridge University Press

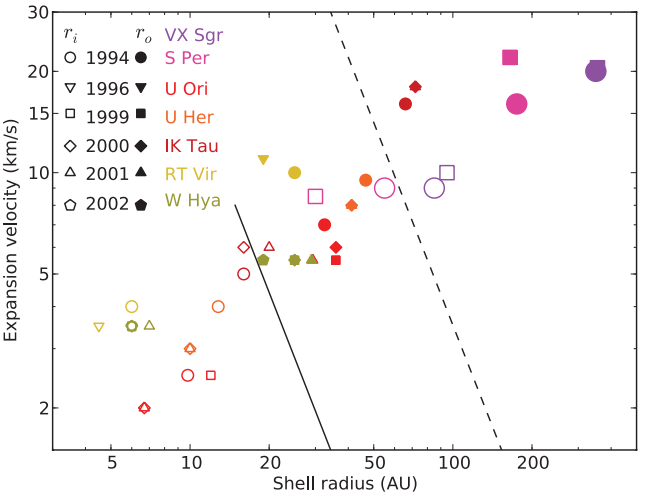

Figure 2. Inner and outer H_2O maser shell limits for 7 stars, showing consistent increase of velocity with radial separation from the star. The solid and dashed lines show the escape velocities for 1 and 20 $M_\odot$ stars, respectively.

Elitzur *et al.* (1992) predicted that unsaturated, 'amplification bounded' maser beaming from spherical clouds produces maser components of measured size s which appears smaller near the line centre, according to the relationship $s_\nu \propto 1/\sqrt{\ln(I_\nu)}$ where I is the flux density at frequency ν. This relationship was investigated for several epochs of observation of 22-GHz masers around five evolved stars (Richards *et al.* 2011). s is inversely proportional to I for most observations of S Per, RT Vir and IK Tau but a more random scatter or an increase in size of the brightest masers was seen in a minority of cases, particularly for U Her and U Ori. The latter behaviour is consistent with 'matter bounded' beaming from shocked slabs. There is additional evidence that these objects might be more prone to shocks. Anomalous OH 1612-MHz flares have been detected (Pataki & Kolena 1974; Chapman & Cohen 1985; Etoka & Le Squeren 1997). Moreover, U Her and U Ori have regular optical pulsations, amplitudes 5–6 magnitudes, in contrast to e.g. RT Vir, with amplitude < 2 mag or S Per, amplitude < 4 mag although it is an RSG. These results are summarized in Fig. 3.

2.3. *Cloud size and mass loss from the stellar surface*

The size of 22-GHz H_2O maser clouds is proportional to the stellar radius (as measured by NIR interferometry), Fig. 4 (see Richards *et al.* 2012 for references). Although there is a tenfold range in $R_\star$, from the smallest AGB stars to the largest RSG, in each case, if the maser cloud size was scaled back to the star assuming radial expansion, the birth size would be 5–10% $R_\star$. This is not what would be seen if cloud size was determined by local micro-physics, such as cooling related to dust formation, since this would operate on the same scale for all stars. Some stellar property must determine the cloud size. Models by Chiavassa *et al.* (2010) and Freytag & Höfner (2008) produce convection cells on suitable scales and optical/IR interferometry (Haubois 2009) shows stellar surface features which are consistent with these models.

VLTI observations reveal an AL_2O_3 layer at the stellar surface, the depth and temperature of which depend on stellar phase (Wittkowski *et al.* 2007; Wittkowski, Cotton these proceedings). These could provide the nuclei for silicate dust condensation at larger radii. Coordinated VLBA imaging of SiO masers shows that these are generally

https://doi.org/10.1017/S1743921312006977 Published online by Cambridge University Press

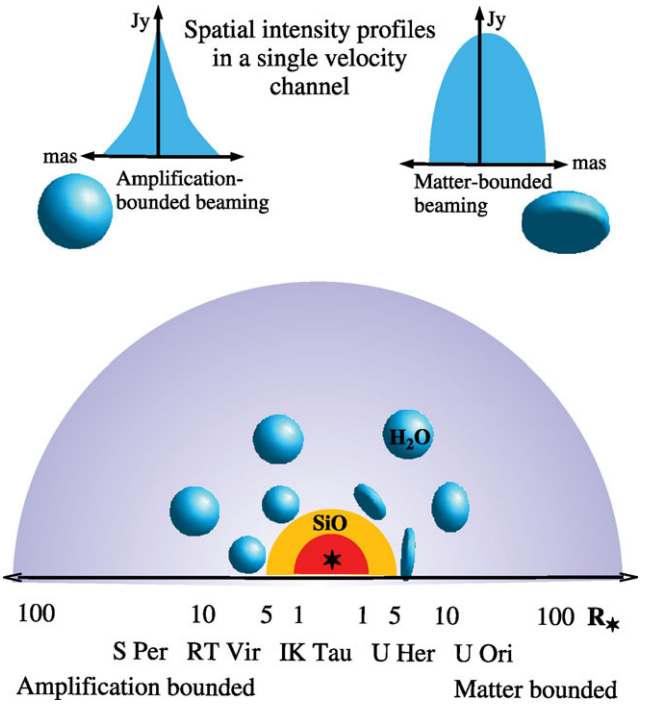

Figure 3. Cartoon (not to scale) summarising the inferred nature of H_2O maser clumps. Their appearance is mostly consistent with random, on average spherical clouds, but some clouds, round some CSEs, show properties consistent with shock-flattening.

brightest during the first part of the stellar phase, as predicted by Gray *et al.* (2009) and this technique could be used to show any link between dust production and enhanced acceleration.

2.4. *SiO masers tracing conditions near the star*

Comparisons between models and observations of SiO maser variability, the relative locations of the various transitions and other properties are also presented by Assaf, Cotton, Gonidakis, Ramsted and Richer (these proceedings), and so I will not repeat the wealth of SiO research undertaken in the last 5 years. There has been some success e.g. Soria-Ruiz *et al.* (2007) but also discrepancies such as the coincidence of $v = 2$ and $v = 3$ emission (Desmurs, these proceedings). Testing the prediction that many, bright maser spots at early phase become fewer, larger ones is hampered by the resolution of the VLBA; up to 90% of the total intensity flux is missing from images of R Cas at 176 pc (Assaf *et al.* 2011; Vlemmings *et al.* 2003) and this effect is likely to be felt out to 500 pc or further. Interestingly, the polarized emission seems to have structure on smaller scales, since some R Cas features appear to be $\gg 100\%$ linearly polarized (Assaf these proceedings).

A few other observational highlights include evidence for disruption of the SiO shell by stellar flares from R Cas. The $v = 1, J = 2 - 1$ emission formed a one-sided arc at one of two epochs observed by Phillips *et al.* (2001); several stellar periods later, Assaf *et al.* (2011) found the $J = 1 - 0$ emission was dominated by an eastern arc during the first stellar cycle monitored, and by a western arc during the second. This behaviour is seen occasionally in some stars at some epochs, but not at all epochs nor in all stars. RX Boo shows an analogously one-sided H_2O shell (Winnberg *et al.* 2008).

https://doi.org/10.1017/S1743921312006977 Published online by Cambridge University Press

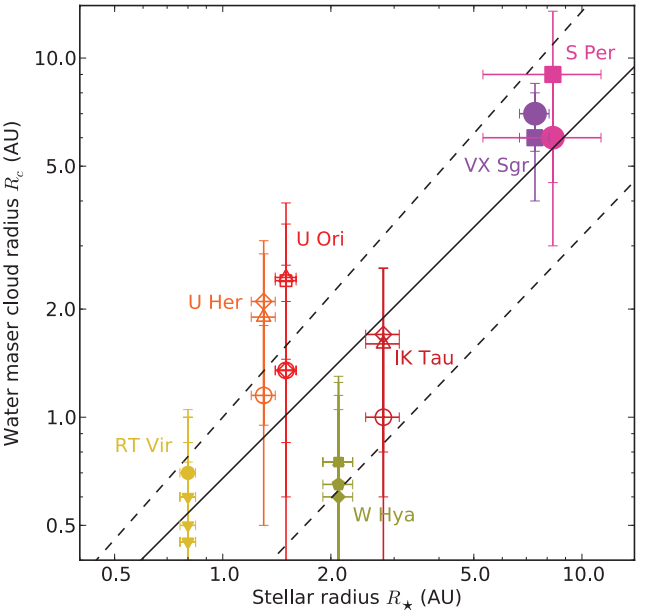

Figure 4. Cloud size

The development of improved calibration techniques (Cotton *et al.* 2011; Kemball & Richter 2011) has led to striking confirmation of the Goldreich *et al.* (1973) model for the behaviour of polarization when the angle between the magnetic field and the line of sight goes through $\arcsin(\sqrt{2/3}$. The fractional linear polarization passes through a minimum and the polarization angle abruptly flips 90°, Fig. 5 (Assaf, Gonidakis these proceedings, Kemball *et al.* 2011). This behaviour is also seen in H_2O masers, covered in the polarization review by Vlemmings (these proceedings).

There is mounting evidence for the Zeeman interpretation of SiO maser polarization, e.g. Richer, these proceedings, but it is still debatable how significant a role magnetic fields play in the mass loss process. Kemball *et al.* (2011) showed that the proper motions of SiO maser clumps round TX Cam are non-linear and not consistently radial, yet the polarization vectors remain approximately orthogonal to the direction of motion. These authors infer that the masers are tracing material accelerated along magnetic field lines, rather than dragging a frozen field in maser clumps (Hartquist & Dyson 1996). In contrast, Matsumoto *et al.* (2008) fitted ballistic trajectories to SiO masers around IK Tau, consistent with pulsation-driven ejection followed by deceleration under the star's gravity. Infall was observed in R Cas (Assaf *et al.* 2011) since faint red-shifted components were seen at several epochs projected against the centre of the SiO ring. These can only be on the near side, since R Cas (radius 13 mas, Weigelt *et al.* 2000) is indubitably optically thick.

An original interpretation of SiO polarization variability was suggested by Wiesemeyer *et al.* (2009), who studied 77 AGB stars with the IRAM 30-m telescope. Of these, only V Cam and R Leo showed quasi-periodic fluctuations of circular polarization, each in just one, individual spectral feature. The variability period was 5–6 hr, and total intensity and linear polarization were not affected. They suggest that this is due to local interaction with the precessing magnetosphere of a Jupiter-like planet. The required magnetic field strength, degree of misalignment of the planetary rotational and magnetic axes, timescale and orbital period/radius, are all consistent with a planet of greater than twice the mass

https://doi.org/10.1017/S1743921312006977 Published online by Cambridge University Press

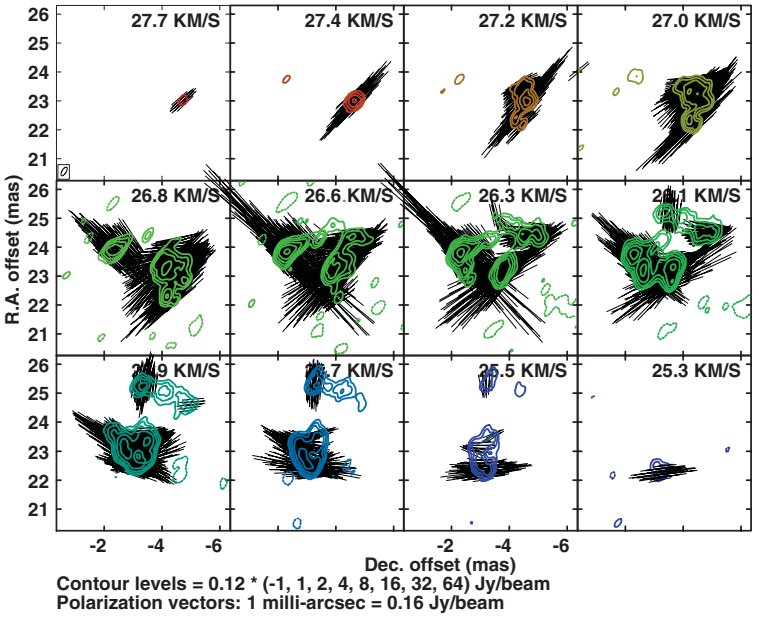

Figure 5. Linear polarization angle of an R Cas SiO feature, showing an abrupt 90° change.

of Jupiter at greater than 3 AU radius. Alternative explanations relying solely on a stellar field either require much too high a field strength at the stellar surface, or cannot explain the locality of the effect, or would be tied to the imperceptibly slow stellar rotation. It would be very interesting to look for similar effects in other monitoring data.

2.5. *Variability in the H_2O and OH mainline maser zone*

The SiO masers at $2-4R_\star$ are very probably strongly affected by stellar pulsations, both shocks and changes in radiation. Conversely, the radiatively-pumped OH 1612-MHz masers at, typically, $\geqslant 100R_\star$, can show variations following the stellar light curve but are otherwise usually stable. 22-GHz H_2O masers, at intermediate distances, are collisionally pumped and highly variable. In some cases, this can be attributed to a discrete spectral and spatial region, likely to be the result of cloud overlap (Kartje *et al.* 1999) e.g. W Hya in 2002 (Richards *et al.* 2012).

Decades of single-dish monitoring has shown long-term variations affecting the whole 22-GHz maser profiles of many stars. These can appear to be correlated with the stellar pulsations, with a lag. Rudnitskii & Chuprikov (1990) suggested that this was due to shocks transmitted through a quasi-stationary layer at $\sim 6-7$ AU. This model was applied to Pushchino data for a number of stars, e.g. R Cas (Pashchenko & Rudnitskii 2004). Shintani *et al.* (2008) monitored 242 evolved stars at 22 GHz using the Iriki telescope and found a correlation between the stellar luminosity and the time lag between stellar and maser maxima, optimised if the time lag was constrained to be greater that half a stellar period by adding one (or potentially more) stellar periods. Such a relationship would be due to the longer periods of higher luminosity stars, which also exert more radiation pressure and possess larger, faster-expanding CSEs. However, the detailed models for the impact of shocks on the 22-GHz masers involve a thin shell expanding at constant velocity, whereas in reality the shells are generally thick and accelerating (Fig. 1). Reid & Menten (1997) and Gray *et al.* (2009) showed that pulsation shock speeds are unlikely

https://doi.org/10.1017/S1743921312006977 Published online by Cambridge University Press

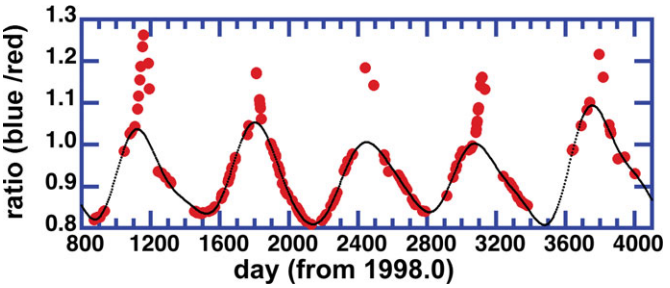

Figure 6. The ratio of the flux densities from the blue- and red-shifted 1612-MHz OH maser peaks of WX Psc, with a curve fitted to the data excluding the cusps overplotted (Lewis 2011).

to exceed $5-7$ km s^{-1} which is smaller than the maximum H_2O maser velocity in most CSEs (Fig. 2).

Rudnitskij (2008) proposed an alternative hypothesis, the effects of a low-mass companion. Intriguingly, one of the stars contributing to this model is R Leo, see Section 2.4 (Wiesemeyer *et al.* 2009). However, proper motion studies show no general rotation in most CSEs. It is possible that both these mechanisms play a limited rôle, with shocks impacting on the inner H_2O masers in some objects e.g. U Her and U Ori, Fig. 3.

Additional potential contributions to variability include changes in the mass loss rate and in dust heating. Evidence for sporadic dust formation comes from Aricebo and Nançay monitoring of WX Psc at 1612 MHz by Lewis (2011). Section 3.1 summarises the expected variability, with the blue-shifted flux density peak leading the red-shifted, so that the ratio is a smooth sinusoid. However, WX Psc shows a sharp cusp at the time of the blue-shifted peak, Fig. 6, due to additional pump photons produced by a thin, enhanced dust shell near the star.

OH masers also exhibit flares which seem generally to be confined to a small region, e.g. Szymczak *et al.* (2010), Wolak *et al.* (2012), Chapman (these proceedings). One of the best-known, *o* Cet, has SiO and fairly weak H_2O masers, but OH appears rarely, only seen around the time of optical maxima on a few occasions. The best-observed previous event was reported by Gerard & Bourgois (1993). The most recent flare (noticed in Nançay monitoring) started in 2010 and has been imaged using the EVN (Etoka & Diamond 2010). Combined with e-MERLIN astrometry of Mira A and B, this will reveal whether the compact companion has any influence on the occurrence of the flares and what the mechanism is.

Two issues are clear; firstly, that long-term monitoring and wide surveys are invaluable (see e.g. Cho, Kim these proceedings) and secondly, multi-epoch imaging is also required to avoid being misled by sporadic asymmetries and brightness fluctuations (periodic or localised).

3. Distance measurements

3.1. *Phase-lag*

OH 1612-MHz shells around OH/IR stars can be several light-weeks in diameter. The maser pump requires 53 μm emission from dust which waxes and wanes depending on the stellar period. Thus, the maser intensity follows the stellar light curve, but we detect the brightening of the blue-shifted peak before that of the red-shifted peak, leading to a sinusoidal variation in the red-blue flux density ratio. Comparing this phase-lag with the angular diameter of a thin, spherical shell gives the distance. However, there were

https://doi.org/10.1017/S1743921312006977 Published online by Cambridge University Press

large discrepancies between early measurements (Herman & Habing 1985; van Langevelde *et al.* 1990) probably because the maser shells were neither thin nor spherical. For example, MERLIN imaging shows that OH 26.5+0.6 is a prolate spheroid, elongated along he magnetic field axis (Etoka & Diamond 2010). Its phase-lag measurements are discussed by Engels (these proceedings), who is leading a campaign (using Nançay, the EVN, e-MERLIN and the EVLA) to obtain adequately complex models to determine the distances to a large sample of OH/IR stars.

3.2. *VLBI parallax*

VERA, the VLBA and the EVN have been used to measure the parallax of many evolved stars as well as star-forming regions (e.g. review by Reid, these proceedings). Individual maser features were tracked by e.g. Vlemmings & van Langevelde (2007), providing distances accurate to 10% or better, in some cases differing by $\sim 30\%$ from *Hipparcos* positions for objects within a few hundred pc and even more for remoter stars.

Statistical parallax – measuring the motion of the centroid of a group of masers – has been used at the distance of the Galactic centre and further. Implications for Galactic dynamics and understanding populations are discussed by Choi, Honma and Oyama (these proceedings) and Whitelock *et al.* (2008) has recalibrated the period-luminosity relationship for Miras using parallax results. The consequences for the classification of individual objects can be very significant, see Imai, Zhang (these proceedings). For example, IRAS 22480+6002 had a dynamical distance of 5 kpc but is actually at 1 kpc, reclassified as an unusual Population II supergiant (Imai *et al.* 2008). IRC-10414 'moved' from 0.7 to > 2 kpc (Maeda *et al.* 2008), thus trebling the proper motion velocities of its masers and turning a gentle outflow into a water fountain.

4. Asymmetry, binarity and post-AGB evolution

These topics are covered by Vlemmings, Amiri, Desmurs, Gomez and Suarez (these proceedings); I briefly note some of the surprises emerging at the meeting. Amiri *et al.* (2011) describe very clearly the distribution of OH and H_2O masers in some water fountain sources. OH12.8-0.9 fits nicely to a biconical model for the OH masers surrounding a relatively young H_2O jet; the higher-velocity jet of W43A has suppressed OH masing which is now confined to an equatorial ring. However, the seemingly well-established scenario in which the H_2O masers trace jets at speeds which can exceed 100 km s^{-1} was dealt a blow by Claussen (these proceedings) who reported that one of the twin outflows from IRAS16432-3814 has apparently come to an abrupt stop. Most models assume that binarity is needed to produce the highly collimated, magnetised jets, but since companions have not been detected in many objects it is still possible that a solitary star's core, revealed in the last stages of envelope loss, possesses sufficient angular momentum.

Symbiotic stars are interacting binaries showing the signature of accretion from an extended star, e.g. a Mira, onto a compact main sequence or white dwarf. Optical and higher frequency lines indicate an accretion disc and some undergo periodic nova outbursts or even possess a jet, e.g. R Aqr, one of only 3 such objects in which masers had previously been detected (Ivison *et al.* 1994). These are D-type symbiotics, showing evidence for dust but S-types have bright stellar spectra and in all cases there is evidence for an ionised nebular e.g. radio continuum. Amazingly, a survey by Cho & Kim (2010) of 47 symbiotics revealed that 19 (including one S-type) have SiO and/or H_2O masers. This suggests that dense, shielded clumps persist despite the hostile environment, which has implications for the survival of molecular material in AGB winds generally.

https://doi.org/10.1017/S1743921312006977 Published online by Cambridge University Press

5. Meermasers

High-resolution imaging of the well-known 43, 22, and 1.6 GHz circumstellar masers, e.g. Fig. 1, has shown that these are generally found at increasing distances from the star, consistent with their decreasing excitation temperatures from species to species. However, the location of different transitions of the same species, e.g. SiO, does not always agree with predictions. Either the maser theory is incomplete or the CSE structure is more clumpy and inhomogeneous than has so far been modelled. Occasional detections of excited OH transitions (e.g. 6 and 1.7 GHz, Desmurs *et al.* 2010) around post-AGB or later stars, suggest pockets of conditions similar to star-forming regions, perhaps associated with collimated outflows, but these detections are very rare and seem to be transient. Millimetre and sub-mm masers, covered in this meeting by Menten, Perez Sanchez, Vlemmings and Wooten, are predicted to sample a wider range of physical conditions, and hence to provide much better constraints on the detailed temperature and density structure of the wind. ALMA will provided unprecedented imaging capability, producing great advances in at least three areas:

(*a*) C-rich star CSEs will be imaged in as good detail as O-rich, using lines such as HCN and SiS (first reported masing by Lucas & Cernicharo (1989) and Fonfría Expósito *et al.* (2006), respectively).

(*b*) Multiple H_2O transitions will constrain on the conditions from $\sim 5 - 100R_\star$, in particular straddling the dust formation zone. An equally rich range of SiO lines will allow even further refinement of detailed models for conditions close to the star.

(*c*) Simultaneous detection of the star, dust and thermal lines will settle many old arguments about expansion mechanisms, maser pumping and chemistry.

Herschel is already providing valuable data, such as overall H_2O abundances and the ortho:para ratio (e.g. IK Tau, Decin *et al.* 2010), and tests of predictions for maser lines. 13 predicted masing H_2O lines have been detected above 1 THz in VY CMa (Royer *et al.* 2010), and new OH masers should also appear in this range.

Acknowledgements

I thank the many people who contributed ideas, information and figures to this review, including Marcello Agundez, Nikta Amiri, Khudhair Assaf Al-Muntafki, Valentin Bujarrabal, Dieter Engels, Sandra Etoka, Malcolm Gray, Liz Humphreys, Murray Lewis, Mikako Matsuura, Huib van Langevelde, Georgij Rudnitskii, Wouter Vlemmings, Markus Wittkowski and Jeremy Yates. I apologise for any ommissions or inaccuracies which are entirely mine.

References

Amiri, N., Vlemmings, W., & van Langevelde, H. J. 2011. *A&A*, **532**, A149.
Assaf, K. A., Diamond, P. J., Richards, A. M. S., & Gray, M. D. 2011. *MNRAS*, **415**, 1083.
Bains, I., Cohen, R. J., Louridas, A., Richards, A. M. S., Rosa-Gonzaléz, D., & Yates, J. 2003. *MNRAS*, **342**, 8.
Bowen, G. H. 1988. *ApJ*, **329**, 299.
Chapman, J. M. & Cohen, R. J. 1985. *MNRAS*, **212**, 375.
Chapman, J. M. & Cohen, R. J. 1986. *MNRAS*, **220**, 513.
Chen, X., Shen, Z.-Q., Imai, H., & Kamohara, R. 2006. *ApJ*, **640**, 982.
Chiavassa, A. *et al.* 2010. *A&A*, **511**, A51.
Cho, S.-H. & Kim, J. 2010. *ApJ*, **719**, 126.
Cotton, W. D., Ragland, S., & Danchi, W. C. 2011. *ApJ*, **736**, 96.
Danchi, W. C., Bester, M., Degiacomi, C. G., Greenhill, L. J., & Townes, C. H. 1994. *AJ*, **107**, 1469.
Decin, L., *et al.* 2010. *A&A*, **521**, L4.

https://doi.org/10.1017/S1743921312006977 Published online by Cambridge University Press

Desmurs, J.-F., Baudry, A., Sivagnanam, P., Henkel, C., Richards, A. M. S., & Bains, I. 2010. *A&A*, **520**, A45.
Elitzur, M., Hollenbach, D. J., & McKee, C. F. 1992. *ApJ*, **394**, 221.
Etoka, S., & Diamond, P. J. 2010. *MNRAS*, **406**, 2218.
Etoka, S., & Le Squeren, A. M. 1997. *A&A*, **321**, 877.
Fonfría Expósito, J. P., Agúndez, M., Tercero, B., Pardo, J. R., & Cernicharo, J. 2006. *ApJLett.*, **646**, L127.
Freytag, B., & Höfner, S. 2008. *A&A*, **483**, 571.
Gerard, E., & Bourgois, G. 1993. Page 365 of: A. W. Clegg & G. E. Nedoluha (ed), *Astrophysical Masers*. Lecture Notes in Physics, Berlin Springer Verlag, vol. 412.
Goldreich, P., Keeley, D. A., & Kwan, J. Y. 1973. *ApJ*, **179**, 111.
Gray, M. D., Wittkowski, M., Scholz, M., Humphreys, E. M. L., Ohnaka, K., & Boboltz, D. 2009. *MNRAS*, **394**, 51.
Hartquist, T. W. & Dyson, J. E. 1996. *AP&SS*, **245**, 263.
Haubois, X. *et al.* 2009. *A&A*, **508**, 923.
Herman, J., & Habing, H. J. 1985. *A&AS*, **59**, 523.
Imai, H., Fujii, T., Omodaka, T., & Deguchi, S. 2008. *PASJ*, **60**, 55.
Ivison, R. J., Seaquist, E. R., & Hall, P. J. 1994. *MNRAS*.
Kartje, J. F., Königl, A., & Elitzur, M. 1999. *ApJ*, **513**, 180.
Kemball, A. J., & Richter, L. 2011. *A&A*, **533**, A26.
Kemball, A. J., Diamond, P. J., Richter, L., Gonidakis, I., & Xue, R. 2011. *ApJ*, **743**, 69.
Lewis, B. M. 2011. Page 629 of: F. Kerschbaum, T. Lebzelter, & R. F. Wing (ed), *Why Galaxies Care about AGB Stars II*. ASP Conference Series, vol. 445.
Lucas, R. & Cernicharo, J. 1989. *A&A*, **218**, L20.
Maeda, T. *et al.* 2008. *PASJ*, **60**, 1057.
Matsumoto, N. *et al.* 2008. *PASJ*, **60**, 1039–.
Murakawa, K., Yates, J. A., Richards, A. M. S., & Cohen, R. J. 2003. *MNRAS*, **344**, 1. M+03.
Pashchenko, M. I., & Rudnitskii, G. M. 2004. *Astronomy Reports*, **48**, 380.
Pataki, L., & Kolena, J. 1974. *Bull. Am. astr. Soc.*, **6**, 340.
Phillips, R. B., Sivakoff, G. R., Lonsdale, C. J., & Doeleman, S. S. 2001. *AJ*, **122**, 2679.
Reid, M. J., & Menten, K. M. 1997. *ApJ*, **476**, 327.
Richards, A. M. S., Yates, J. A., & Cohen, R. J. 1999a. *MNRAS*, **306**, 954.
Richards, A. M. S., Yates, J. A., Cohen, R. J., & Bains, I. 1999b. Page 315 of: Le Bertre, T, Lèbre, A, & Waelkens, C (eds), *IAU Symp. 191: Asymptotic Giant Branch Stars*. ASP.
Richards, A. M. S., Elitzur, M., & Yates, J. A. 2011. *A&A*, **525**, A56.
Richards, A. M. S. *et al.* 2012. *A&A*. in prep.
Royer, P. *et al.* 2010. *A&A*, **518**, L145.
Rudnitskii, G. M., & Chuprikov, A. A. 1990. *Soviet Astronomy*, **34**, 147.
Rudnitskij, G. M. 2008. *Journal of Physical Studies*, **12**, 1301.
Shintani, M. *et al.* 2008. *PASJ*, **60**, 1077.
Soria-Ruiz, R., Alcolea, J., Colomer, F., Bujarrabal, V., & Desmurs, J.-F. 2007. *A&A*, **468**, L1.
Szymczak, M., Wolak, P., Gérard, E., & Richards, A. M. S. 2010. *A&A*, **524**, A99.
van Langevelde, H. J., van der Heiden, R., & van Schooneveld, C. 1990. *A&A*, **239**, 193.
Vlemmings, W. H. T., & van Langevelde, H. J. 2007. *A&A*, **472**, 547–533.
Vlemmings, W. H. T., van Langevelde, H. J., Diamond, P. J., Habing, H. J., & Schilizzi, R. T. 2003. *A&A*, **407**, 213–224.
Weigelt, G. *et al.* 2000. Page 617 of: P. Léna & A. Quirrenbach (ed), *SPIE Conference Series*, vol. 4006.
Whitelock, P. A., Feast, M. W., & van Leeuwen, F. 2008. *MNRAS*, **386**, 313.
Wiesemeyer, H., Thum, C., Baudry, A., & Herpin, F. 2009. *A&A*, **498**, 801.
Winnberg, A., Engels, D., Brand, J., Baldacci, L., & Walmsley, C. M. 2008. *A&A*, **482**, 831.
Wittkowski, M., Boboltz, D. A., Ohnaka, K., Driebe, T., & Scholz, M. 2007. *A&A*, **470**, 191.
Woitke, P. 2006. *A&A*, **460**, L9.
Wolak, P., Szymczak, M., & Gérard, E. 2012. *A&A*, **537**, A5.
Yates, J. A., & Cohen, R. J. 1994. *MNRAS*, **270**, 958.